Mechatronics And Robotics Society at the University of Virginia

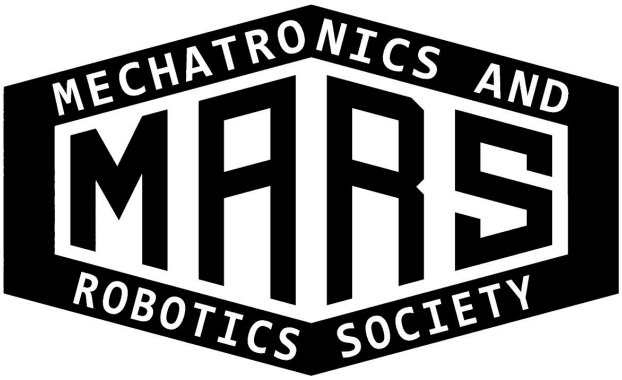

2018 Systems Engineering Paper

School:
University Of Virginia

Team Members:
Henry Spece
Samreen Islam
Cassie Willis
Haley Finegan
Ian Wnorowski
Daniel Chen
Shreejan Gupta
Kendall Nicole Timmons
Cristion Oliphant
Robert Pierce
Hua Uehara
Cesar Roucco
Maria Contreras
Leslie Cueva
Assad Aijazi

Faculty Advisor:
Daniel Quinn

The faculty advisor has reviewed this document:

Dan Quinn

Systems Design and Implementation of HoosMining Robot

Abstract **- The HoosMining team in the Mechatronics and Robotics Society (MARS) is dedicated to the education of its members in the fields of mechanical engineering, electrical engineering, computer engineering, and computer science by means of the construction of a Martian Rover, the participation and promotion of various local events, and the participation in the NASA Robotic Mining competition. The NASA Robotic Mining Competition is an inter-university competitive event intended to aid NASA in the design of autonomous robots for the collection and processing of martian subterranean ice by means of a mock martian mining operation held on simulated martian terrain. A proposed solution to the Martian colonization design problem involves sending a fleet of autonomous robots to the surface to mine the ice known to be present beneath the martian surface because resources such as drinking water and hydrogen will not be readily available to potential martian colonists on arrival. With the intent of partially outsourcing the design of these rovers, NASA has sponsored a competition amongst universities by means of which students may compete and collectively participate in a nation-wide design process. For this year's competition, the HoosMining team in the Mechatronics And Robotics Society at the University of Virginia has improved upon the martian rover design used in previous competitions, resulting in a versatile, rugged, and compact system capable of sifting large quantities of ice from the martian soil and successfully delivering it to a base station.**

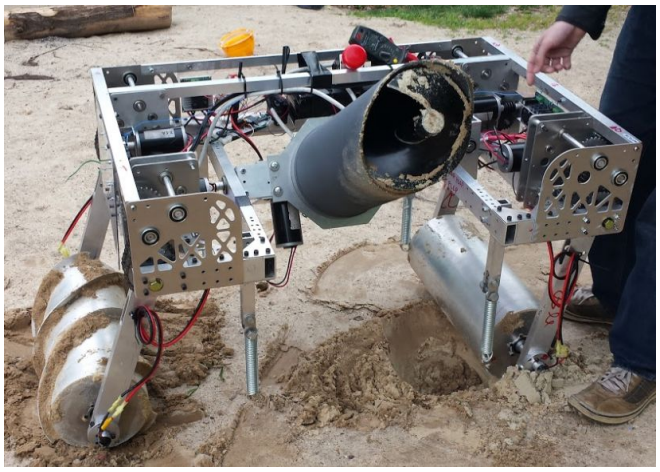

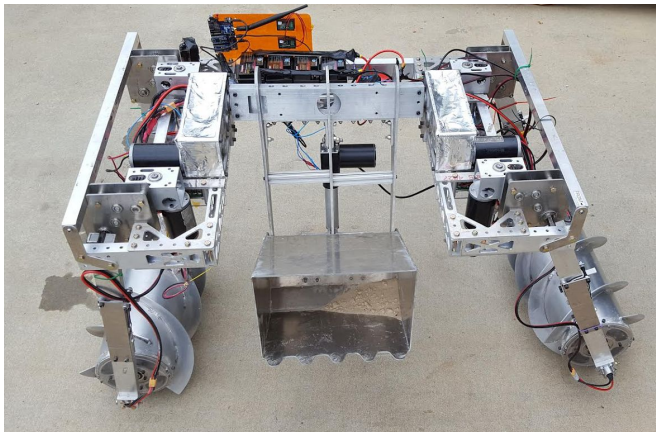

Figure 0. 2016 iteration of Hephermes (top), 2017 iteration of Hephermes (bottom)

Table of Contents

Introduction

Interplanetary colonization continues to be one of the greatest modern engineering challenges. The planet Mars, Earth's next-door neighbor, is one of the first of humanity's stepping stones towards the outer reaches of space, but the problem of colonization of the Red Planet remains unsolved with currently available technology. Among the many challenges faced when attempting to create a permanent martian settlement is that of procuring water and fuel for an eventual return journey to Earth. The currently proposed solution is to send a fleet of rovers ahead of potential colonists capable of mining ice from beneath the soil on Mars and deliver it for processing at a base station. When astronauts finally land, water will be readily available to drink, and the hydrogen and oxygen may be separated to fuel the rocket required for the return journey.

It is not immediately clear what the best design for a martian mining rover would look like, but through the combined efforts of a number of competitive university teams, it may be possible to outsource components of the design and generate innovative ideas which could be seen in future missions. This paper aims to document the systems engineering design process undergone by the HoosMining team in the Mechatronics And Robotics Society (MARS) at the University of Virginia to create Hephermes, a mobile mining robot capable of navigating rough, sandy, terrain and excavating the Martian soil.

Problem Definition

The NASA robotic mining competition arena consists of a 3.8m by 7.4m sand-box, filled 30cm deep at the bottom with a mix of gravel and BP-1 (a fine sand made from crushed basalt), and an additional 30 cm of BP-1 only. Additionally, the field will contain a number of obstacles such as craters and boulders.

Robots participating in the competition must be able to excavate and deliver to a collection bin at least 1 kg of the subsurface gravel, and will be scored based on amount of gravel collected, weight, dust tolerance, autonomy, documentation, and a number of other factors relevant to the design of actual martian robotic systems.

Deliverables

The HoosMining team has outlined the following deliverables for the NASA RMC 2018:

1. A partially autonomous integrated robot with gravel excavating and regolith sifting capabilities
2. A wireless communication protocol between the robot and the controller
3. A systems engineering paper outlining the robot build process and robot features
4. An outreach project report exhibiting the outreach activities conducted
5. A proof of life video exemplifying robot locomotion and excavation

Systems Engineering Design Process

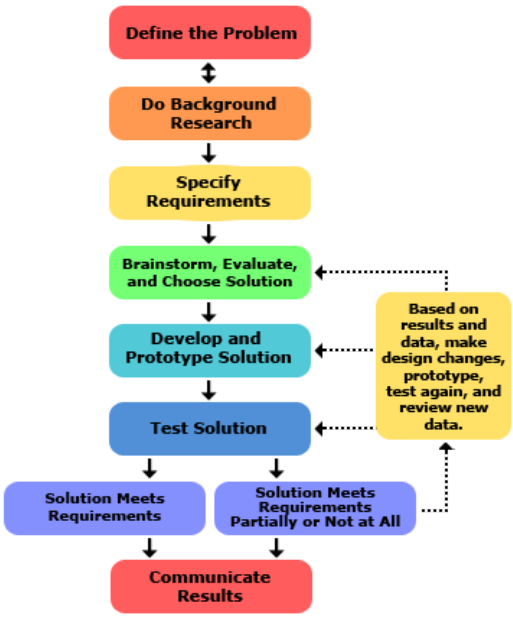

Figure 1. Engineering Design Process[1]

The team employs basic engineering design principles to design, build and integrate the

Table 1. Decision Matrix for Bucket or Auger Design

Factor	*Weight*	*Bucket*	*Score*	*Auger*	*Score*
Completion Time	0.9	1.0	0.9	0.3	0.27
Weight	0.8	1.0	0.8	0.7	0.56
Budget	0.8	1.0	0.8	0.4	0.32
Stability	0.7	0.7	0.49	1.0	0.7
Optimization	0.7	1.0	0.7	0.8	0.56
Gravel Potential	0.7	0.7	0.49	1.0	0.7
On-Load Rate	0.6	0.4	0.24	1.0	0.6
Off-Load Rate	0.6	1.0	0.6	0.7	0.42
Power Consumption	0.5	1.0	0.5	1.0	0.5
Simplicity	0.4	0.6	0.24	1.0	0.4
Autonomous Integration	0.4	0.6	0.24	1.0	0.4
Maneuverability	0.4	0.6	0.24	1.0	0.4
Storage Capacity	0.3	1.0	0.3	0.8	0.24
Regolith Retention	0.3	1.0	0.3	0.6	0.18
TOTAL			**6.84**		**6.25**

HoosMining robot. The well-established engineering design process is outlined in the figure 1. The HoosMining team undertakes the following steps to organize the robot build process- problem definition, requirements specification, brainstorming, prototyping, evaluation, testing and reiteration. This process is adhered to for every subsystem design as outlined throughout this paper.

Given the dramatic change in point distributions this competition season, where collection of BP-1 receives zero points, HoosMining had to make pivotal design decisions before school started in order to start brainstorming with new members at the beginning of the school year. By far, the biggest design decision made was regarding the excavation sub-system. The team decided to compete with the bucket excavating system (average collection of 0.3kg of gravel) instead of the auger system (average collection of 3 of kg of gravel) used two competition seasons ago. The auger system performs much better within the new rules; however, exchanging the bucket system with the auger system would require hundreds of hours in the machine shop: redesigning gearboxes, manufacturing parts, and completing massive lean analysis on our already 79 kg excavator robot. It was decided that with only four returning members, and an unknown number of new recruits for the upcoming build season, that focus needed to be on optimizing the bucket's gravel digging abilities with new digging tactics and add-on mechanisms. Table 1 exhibits the decision matrix of several factors considered when determining which excavator design should be chosen.

Concept Development

Objectives

The team's primary objective this year was to implement partial autonomy so that the robot could autonomously traverse the obstacle field. Additionally, the team aimed to make minor modifications to the mechanical design of the robot to improve efficiency of locomotion, excavation and to reduce weight of the robot to facilitate smoother autonomy implementation.

Design Philosophy

The team's general design philosophy emphasizes on learning and personal growth through the design and development of a Martian mining robot. With that thought in mind, team members brainstorm, prototype and develop ideas that sometimes may not result in feasible implementation but serve as learning experiences and contribute to the reservoir of knowledge of

the team as a whole so that members can learn from each others' mistakes and successes.

System Architecture

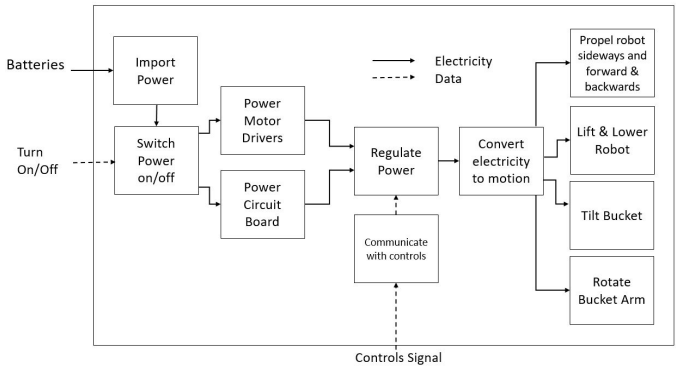

Figure 2. System Architecture of HoosMining Excavator

Background/Initial Design

The solution to the problem posed by the NASA robotic mining competition used in previous years is a robot frame consisting of multiple joints, rotating screws for propulsion, and a front-loading excavator on the front for collection of martian soil (Figure 3).

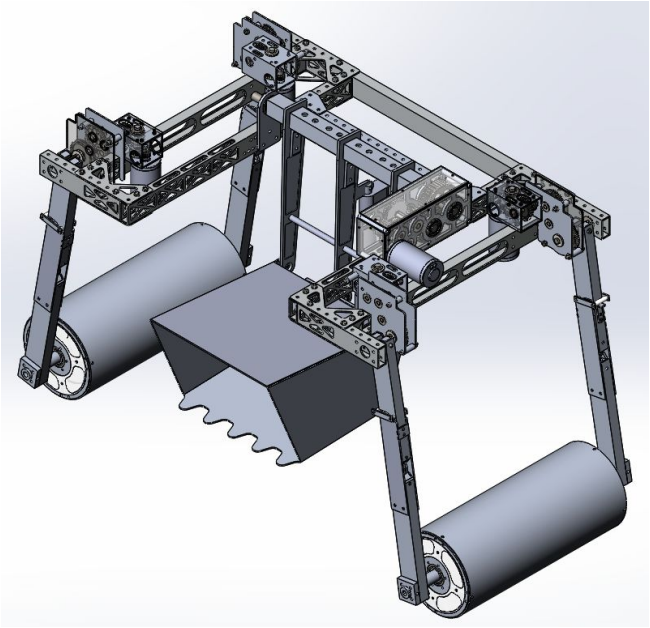

Figure 3. CAD of Excavator

Advantages of the design are the following:

1. The design meets all minimum system requirements as defined in the NASA RMC rules and rubrics (weight, sealing, safety, regolith simulant delivery etc)
2. The rover is very maneuverable, capable of shifting its center of gravity to accommodate rough terrain
3. The robot is capable of recovering from a tip at any angle
4. A collapsing frame allows the robot to occupy a large footprint when deployed while still meeting necessary size requirements when inspected before a competition match
5. Screw propulsion combined with strategic use of the robot's weight allows for high penetration force when digging

Unfortunately, many issues with the design also needed to be addressed, and the design objective for this year was to fix the following problems without compromising the above advantages of the existing design:

1. The center of mass is quite high, reducing resistance to tipping seen in previous system designs
2. The robot's ability to collect large quantities of regolith simulant in previous years is irrelevant to the current competition objective of collecting as much subsurface gravel as possible
3. Gearboxes which drive the rotation of the screws used for robot propulsion are capable of damaging themselves, and experimentally have been shown to do so frequently
4. When unfolding, there is a chance that the frame does not "lock" into place, which is a requirement for the robot to be stable later, while moving
5. Many of the electrical cables used to distribute power are not mounted as safely or securely as is desired
6. The robot is unnecessarily heavy

7. The mounting assembly for the "legs" of the robot has a limited service life, and requires frequent replacement
8. The circuit board controlling the robot had components which caused incorrect voltage levels at multiple power and signal points.

Design Decision

Work this year focused primarily on the redesign of several system-critical components, and the integration of additional sensors required for autonomous operation of the robot. Due to the success and maneuverability of the previous years' design, the overall structure of the robot's appearance and mode of operation was not significantly modified for this year's competition.

Mechanical Design

After ideation and preliminary prototyping, each mechanical subsystem was designed in SolidWorks before being manufactured. The overall architecture and component interactions of the mechanical system of the robot is shown in Figure 4 below.

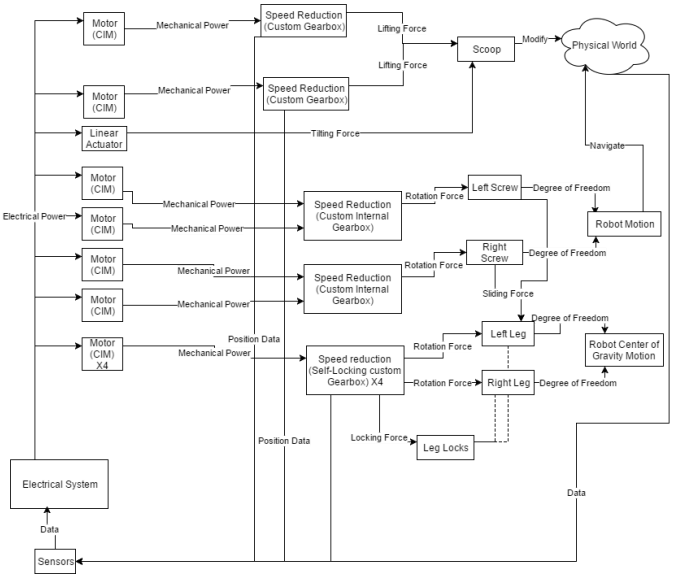

Figure 4. Mechanical Design Diagram

Screw Gearbox Redesign

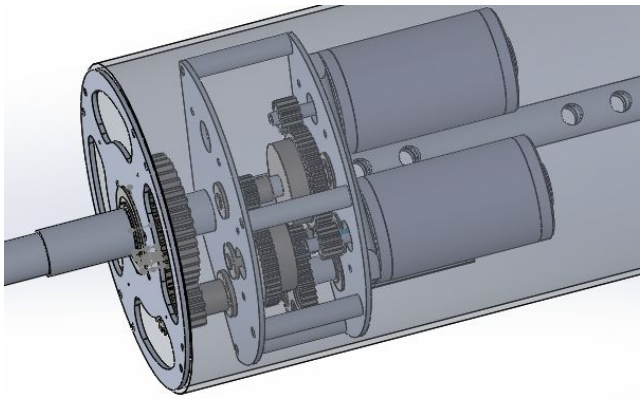

Figure 5. CAD of Screw Gearbox Redesign

In light of systematic design concerns over the gearboxes which drive the robot's screw propulsion, it was decided that the design of new gearboxes should be undertaken from scratch. While the initial design involved a pair of gearboxes per screw, resulting in the issue of unexpected loading on the main output shaft, a new design would consist of a single gearbox design per screw, each with a pair of motors driving the input shaft and a single output shaft. Only a single gear-train would then be necessary, as opposed to a pair of gear trains, and the motors could only "fight" each other in the early gear reduction stages, theoretically reducing the resulting internal torques. Meanwhile, if the resulting design is assumed to be the weight of the initial design, then larger, heavier gears may be used, since there is only a single gear train per screw.

In the case of the screw-propulsion gearboxes, an iterative design process was undertaken which involved the selection of parts, arrangement in the appropriate combinations, preliminary CAD design, and a return to component selection. The previous gearbox design was used as a guideline, simultaneously as inspiration for a number of design ideas and as a set of constraints, including weight, size, and power output. The final design of the screw propulsion gearbox may be seen in Figure 5.

Leg Clamp Redesign

A solution to the "leg" mounting assembly issue was devised which would involve the inclusion of a thin hexagonal "sleeve" which would pass over the steel output shaft prior to the mounting of the compressive "clamp" assembly. While this would not solve the issue of limited service life due to the large torques involved, replacing the small sleeve would be much simpler than the remanufacture of the entire assembly, and would thus be advantageous. The final solution, rendered in Solidworks, may be seen in Figure 6 .

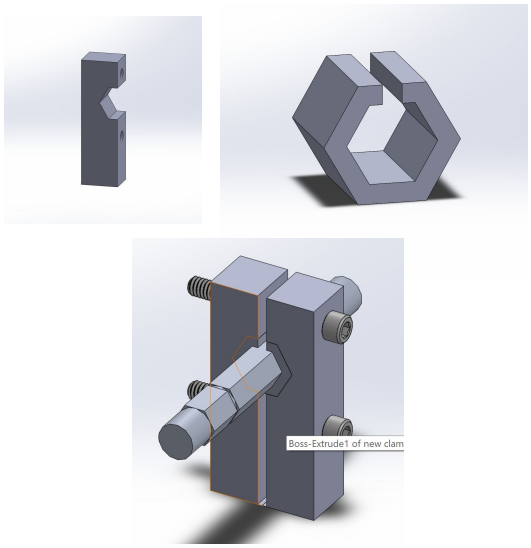

Figure 6. CAD of Leg Clamp

Excavator Modifications

In light of the fact that this year's competition does not score robots based on regolith simulant collected, but only gravel collection, it was necessary to reconsider the front-loading excavator design on this year's robot. After considering a number of design alternatives, it was decided that the conservative approach of minor modifications to the existing excavator design would be the best means of maximizing the gravel collection and delivery. By sifting out all of the worthless regolith simulant with each scoop, the robot can take far more scoops in a single trip to the excavation area with its limited-capacity storage.

A half-inch aluminum mesh for the purpose of sifting was attached to the bucket as a drop-in replacement for the polycarbonate panel already present at the back of the bucket as shown in Figure 7. As a result, any regolith-simulant collected in the bucket will pass through whenever the bucket is lifted, leaving behind only gravel particles above the minimum required particle size.

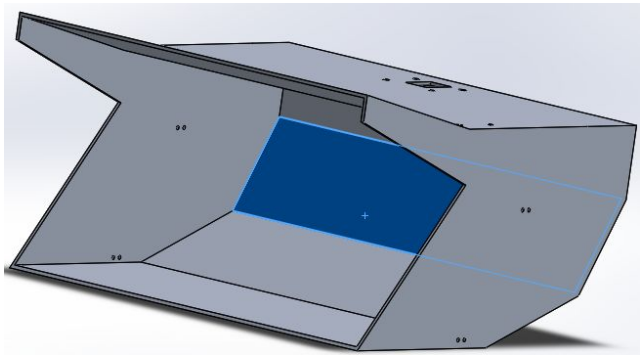

Figure 7. bucket CAD with blue panel replaced by sieve

In order to maximize the efficiency of BP-1 sieved through the excavator to enable optimal gravel collection, the team brainstormed and prototyped a variety of excavator modifications. The modifications were considered with two main goals in mind- to facilitate faster sieving and to facilitate faster digging. The ideas for faster and more efficient sieving of the BP-1 in the bucket comprised of the following ideas:

1. Attaching a motor with an off-kilter weight to the back of the bucket to essentially act as a vibrator that could loosen up the sand for faster sieving
2. Attaching sieves to the sides of the bucket for continuous sieving while digging
3. Attaching a lid to the back of the bucket with a mechanical system of opening and closing the lid to prevent BP-1 from sieving out into the hole that the excavator is currently digging

4. Attaching a shaft with protruding metal blades that break up the BP-1 inside the bucket before the soil reaches the sieve

The primary idea to ensure faster digging involved the installment of a horizontal rotating auger near the opening of the excavator that would pull sand into the bucket at a faster rate than if the bucket was just digging like a regular shovel.

The team is currently in the process of prototyping the vibrator mechanism, sieves on the sides of the bucket, a lid to retain regolith while digging and the horizontal auger for faster digging and expects to have the aforementioned excavator improvements implemented and tested by the time competition arrives.

Mass Reduction

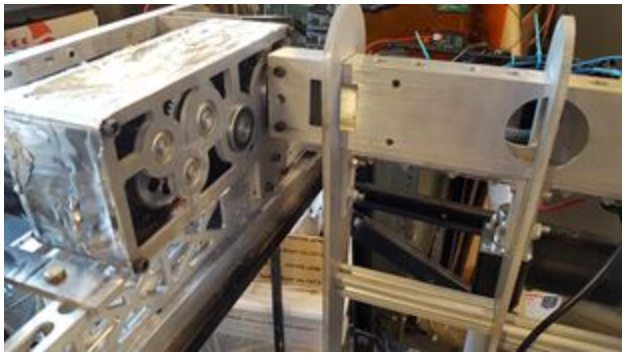

Figure 8. Gearbox for Bucket

Firstly, it was determined that the issue of the height of the robot's center of mass, as well as that of the robot's overall weight could be alleviated somewhat with the removal of heavy components near the top portion of the robot chassis. In particular, one of a pair of gearboxes responsible for the actuation of the central excavator could be removed and replaced with a bearing mount. Since the initial design of the two gearboxes was performed with a high factor of safety (>2) and a number of conservative estimates of material/motor strength, it is expected that the new design will not have any less strength than is needed to lift the correct quantity of regolith-simulant. The sample calculations for the factor of safety of each component in the excavator-lifting subsystem is observed to be greater than 2 as shown in Figure 9. However, with only one gear box the bucket system is no longer self-locking, and the weight of the bucket system is larger than the torque provided by the worm gear within the gear box. Thus, a feedback loop with a potentiometer is needed to control bucket position at all times now, as opposed to only having feedback position control enabled when the bucket is full.

Despite the drawback of requiring constant feedback control on the bucket to retain its position, the removal of one of the bucket-lifting gearboxes, along with the re-design of the screw gearboxes reduced the weight of the robot by 10 kgs. Thus, freeing up weight for excavator innovations.

ITEM	SAFETY FACTOR
Stage 1, Gear 1	32.08
Stage 1, Gear 2	32.45
Stage 2, Gear 1	10.2
Stage 2, Gear 2	9.09
Stage 3, Gear 1	2.86
Stage 3, Gear 2	2.77
Stage 4, Gear 1	3.48
Stage 4, Gear 2	5.36
Stage 5, Gear 1	2.19
Stage 5, Gear 2	2.79
Stage 1 Output Shaft	21.98
Stage 2 Output Shaft	6.3
Stage 3 Output Shaft	2.95
Stage 4 Output Shaft	6.11
Stage 5 Outputs Shaft	2.79
Stage 3 Output Shaft Key	18.07
Stage 4 Ouput Shaft Key	9.04
Stage 5 Output Shaft Key	3.87
Inner Gearbox Plate	2.68
Outer Gearbox Plate	2.86
Support Beam, Vertical Load	3.32
Support Beam, Horizontal Load	4.52
Support Beam, Side Load	2.88

Figure 9. Sample Safety Factor Analysis for Excavator-Lifting

Electronics

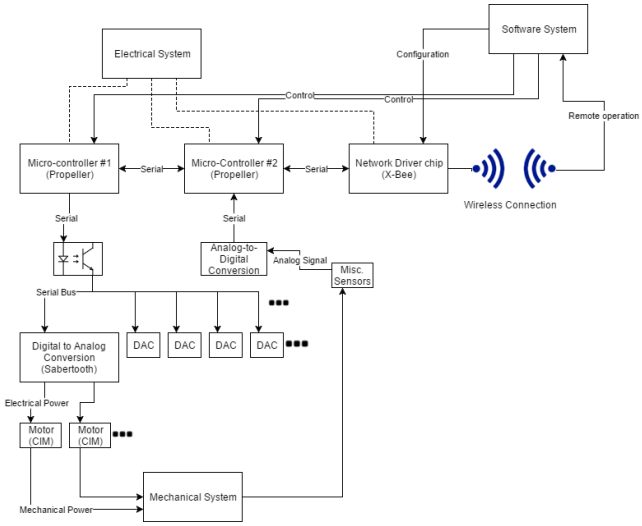

Figure 10. Electrical Systems Diagram

Additional design changes to the mechanical subsystem of the robot were foregone in favor of changes to the electrical and controls subsystems, with the intent of saving undue time and resources. For example, it was decided that harnesses for crucial wiring components along with a new container for the robot electronics board would be designed, as will be detailed in the following sections.

To deal with the voltage levels not meeting required specifications, several elements of the board were redesigned and components such as pull down resistors leading to LEDs that were only used for testing were removed and the design was cleaned and reprinted.

After making the above decisions about the design of the robot's subsystem improvements, individual team members were divided and assigned appropriate design tasks.

Power Distribution Redesign

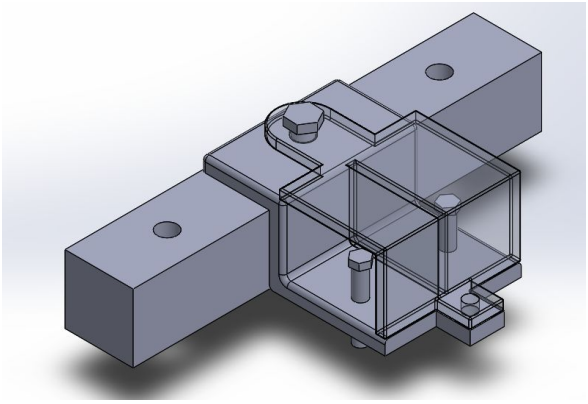

Figure 11. 3D Printed Electrical Hinges CAD

The electrical hinges (Figure 11) were redesigned for accessibility and to condense two mounts into a single hinge. The hinge has separate connection points for both wire sets and contains a divider to ensure that no interaction between the sets occurs. The cube-like design also provides protection from dust contamination on five of six sides.

Electronics-box Redesign

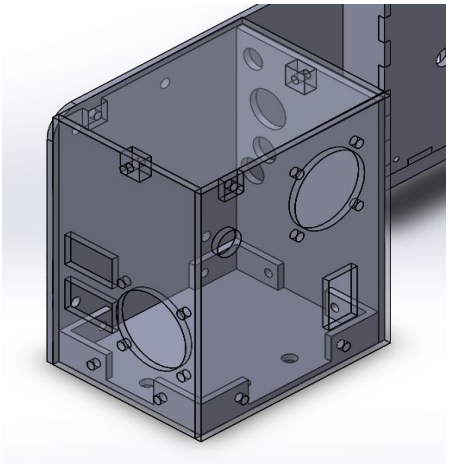

Figure 12. Electronic Box CAD

The electric box (Figure 12) was redesigned to allow easier access to the internal components as well as provide more stability to the structure.

The walls are made from clear polycarbonate material due to its lightweight and translucent properties. The fastening of the box by zip-ties was replaced with screws, and custom 3D printed parts were used for the lid and the base to make for a more dust tolerant design.

Circuit Board Modifications

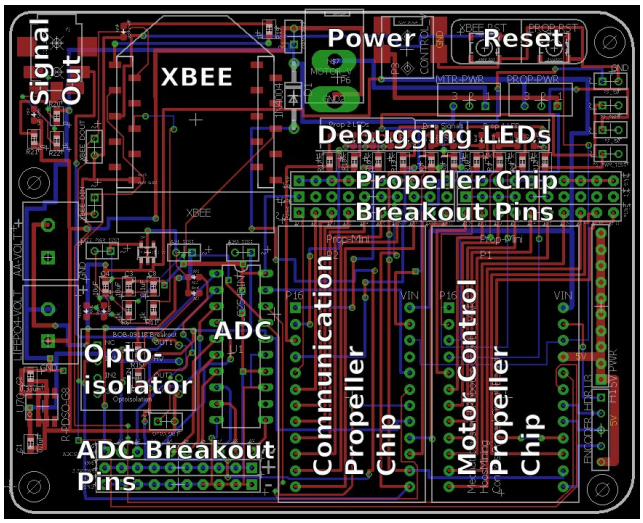

Figure 13. Eagle CAD of PCB

The printed circuit board did not change significantly from the previous year's design. The main change in the board was to remove components that needed to be desoldered from the board before competition last year. These parts were pull up or pull down resistors that connected signal lines to LEDs for signal verification. The resistors were necessary for properly powering the LEDs at the correct voltage, however they had the unintended effect of lowering the voltage of the signal line, which caused the signal to not be strong enough to be read by the receiver. Because these LEDs were only used for verification purposes, the decision was made to remove these resistors and LEDs.

Another change to the PCB was in adding signal lines to the header pins from the Analog to Digital Converter (ADC). Originally, the ADC was not going to be in use for last year's competition and was added to the board so that adding sensors this year and in future years would be easier. This changed only weeks before competition when the team decided to add potentiometers for monitoring torque on the motors. This and the additional sensors added this year meant that wiring from the ADC to the headers needed to be added. The sensors are still connected to the board via headers so that they can easily be changed.

After these changes were made to the design, the board was reprinted and assembled so that a clean version of the board without any external wiring or empty pads could be used for competition.

With those changes in mind, the remainder of the board remained unchanged. To monitor the robot's arm and excavator orientation, potentiometers are used to provide position feedback. Potentiometers were chosen for their ease of integration with the control system on the robot. The position of the potentiometers is converted to a digital value with a TLC2543 twelve-bit, multi-channel ADC. Serial Peripheral Interface (SPI) is used as the communication interface between the ADC and the primary Propeller chip to prompt the measurement of a specific channel and to read back the digital value. The ADC also allows the capability to add multiple sensors with analog output into the chip for use in collecting more data about the robot and its surroundings. The sensors that were specifically added are described later in this report.

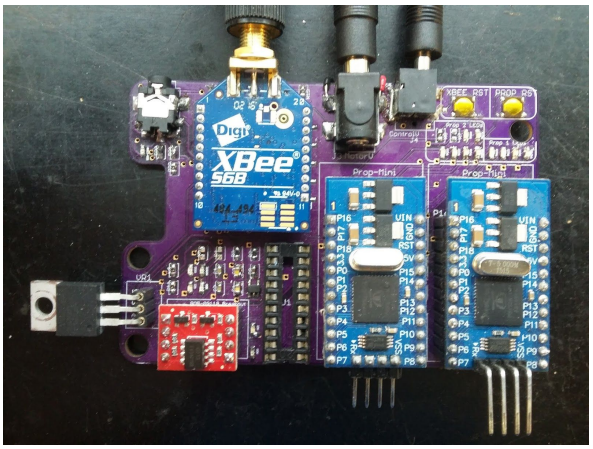

Figure 14. Propeller Microcontroller

Parallax Propeller chips were used for the control system because their parallel architecture allows for eight processes to be executed simultaneously. Examples of processes allocated to individual cores are serial communication, Proportional Integral Derivative (PID) control, and sensor input reading and processing. The serial communication core is used to receive data from the XBee and communicate between the two Propellers. Two Propellers are used to control the robot to make room for future expansions onto the secondary Propeller. The primary Propeller processes commands received from the secondary Propeller through a serial connection, as well as position input from potentiometers on the arms and excavator to determine what motor speeds to send to the Sabertooth motor drivers. The secondary Propeller receives commands from the command server through XBee, and passes the commands to the to the primary Propeller. This allows the free cores in the secondary Propeller to be dedicated to processing data from additional sensors. The data flow can be visualized in Figure 15.

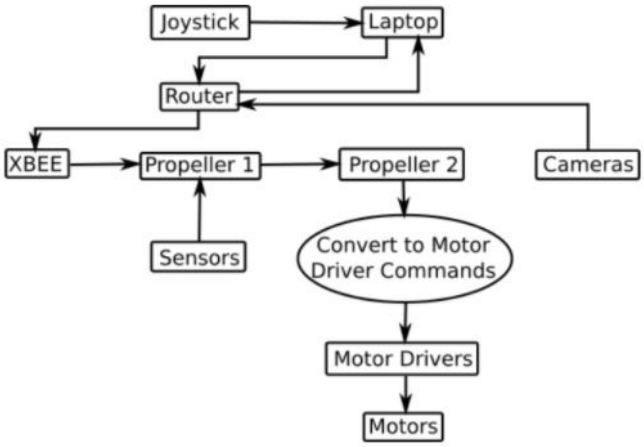

Figure 15: Data flow from controller to motors.

AUTOMATION

Previously, the robot had little to no automated features. The only form of real time feedback control was on the bucket which could hold its position based on the position of the potentiometer and correct itself based on the weight of regolith in the bucket. This year, the team decided to expand on automation and aim for the first tier of partial automation, namely, autonomously crossing the obstacle field. Automation efforts additionally focus on any subsystem that assists in seamless robot locomotion. For example, the issues of the robot frame not locking completely on deployment may be alleviated by the recent addition of limit switches which will detect when the locking mechanism has not closed properly, and adjust the output to the motors correspondingly.

Leg-locking Notification

Figure 16. Leg Lock in locked position

The leg-locking mechanism on the robot serves to increase the height of the robot during the competition run so as to improve flexibility in stance width and contribute to easier reach to the deposit bin. The robot locks its legs into place by resting with its weight on the bucket and extending its legs as far out as possible so as to lock the joint.

In the past, a problem the team frequently ran into with the leg locking mechanism was that one leg (front or back) of each side would lock before the other, after which the robot would operate with an unlocked leg. This would cause the robot movements to be uneven, and distribute stress unevenly between the legs, causing damage over time.

To address this, a limit switch was added to each leg to track the movement of the leg, and make sure that each leg completely locks before stopping the motor. The limit switch is positioned to directly detect when the leg lock becomes active in order to provide feedback on the position of the leg lock. The mount for the limit switch is shown in Figure 17 and the way the leg-locking hinge interfaces with the limit switch is displayed in Figure 18.

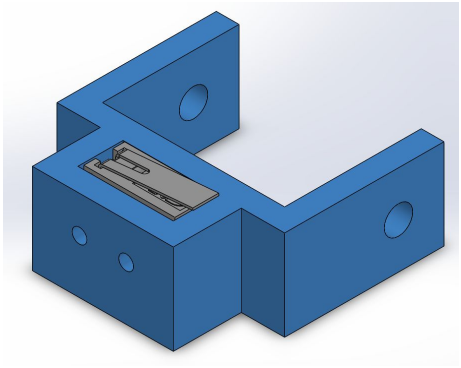

Figure 17. Limit Switch Bracket

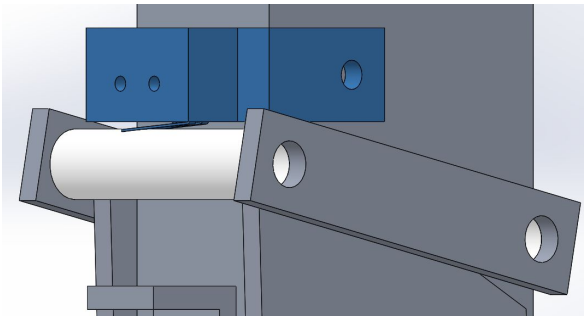

Figure 18. Limit Switch interfacing with leg lock mechanism

Obstacle Detection and Avoidance

Ideation

The team went through several rounds of brainstorming and discussions to determine sensor selection and mounting for obstacle detection. Some ideas that the team went through are listed below:

1. Computer vision for detecting obstacles
2. Computer vision for recognizing a beacon at the deposit bin and gauging relative position of robot on the field
3. Sweeping LIDAR sensors to make a point map of obstacle field which the robot would then traverse
4. IR distance sensors for basic obstacle avoidance

5. Potentiometers attached to the legs and screws to determine distance travelled by the robot
6. Accelerometers to determine the pitch and roll angles of the robot so that it detects when it is about to dip into a crater

Challenges

This year an attempt was made to add object distance recognition into the robot. The robot contains two cameras, which were used to locate the closest object that is near the robot. The program used the OpenCV imaging library with the cameras to keep track of the of the robot's surroundings, and the algorithm took the image from the camera, converted it into grayscale, and used a greedy algorithm to locate the brightest pixel within that image where the closest object should be located. To increase the reliability of this algorithm, the cameras had light sources attached to them so that the camera can read in the reflected light, as well as first converting the image to a grayscale image before analyzing it. Unfortunately, even with these modifications, the algorithm proved too unreliable to detect nearby objects, often getting distracted by brighter objects that are farther away.

Despite the barriers to successful implementation of computer vision on the robot this year, the team has established a platform for computer vision that can be explored for next year's iteration. In light of the lack of optical sensors, the team decided to go with a simplistic approach to obstacle avoidance with unidirectional lidar sensors that would simply detect obstacles like boulders and traverse around them.

Implementation

Due to the unique design of the HoosMining robot, even this simplistic approach faces significant challenges. There are two main ways that the HoosMining robot may be placed in the arena for which sensor configurations would vary:

1. the robot may be placed sideways so that the screws are longitudinally parallel to the obstacle field
2. the robot may be placed facing forward or backward such that the screws are perpendicular to the obstacle field

The HoosMining robot traverses Martian terrain fastest when it is placed in the arena in configuration (1) i.e. when it is strafing side to side. Given that the robot is in the aforementioned configuration in the field, the angle of the legs from a vertical baseline will determine the pitch angle of the lidar sensors and so the sensors will not necessarily be facing horizontally across the obstacle field. Therefore, there must be some mechanism, like a gimbal, that adjusts the pitch angle of the lidar sensor so that its line of sight is as horizontal to the field as possible for it to effectively detect objects of a certain size. The avoidance method in this case would involve driving the robot forward or backward to clear the obstacle. The distance driven forward or backward can not simply be equal to the length of the screw since there is the possibility of detecting additional obstacles in the process of avoiding one.

If the robot is placed in the arena in configuration (2), i.e the robot drives forward or backward, the sensors can be attached to the front of the screws at a specific height such that only large obstacles that the robot cannot easily drive over are detected and avoided. The

avoidance method in this case will involve adjusting the distance between the screws by changing each leg's angle from the vertical i.e taking a wider or narrower stance to avoid the obstacle.

Given the plethora of complications that may arise during autonomous navigation of the robot, the team has ensured that the robot can be switched to manual remote control as necessary in the field.

Software

The primary goals for the robot software is to provide a way for the user to control the motors and the excavator of the robot. The software is comprised of two components, the front end and the back end. The front end includes the Graphics User Interface (GUI) that allows the user to modify the joystick and keyboard that controls the robot, and it communicates with the back end through the transmission of Transmission Control Protocol (TCP) packets. The back end receives the packets and translates them to determine which motors need to be commanded and how they should be operated. Further goals for the robot software aim to integrate feedback from newly installed sensors such as limit-switches for leg-locking, distance data from LIDAR sensors, pitch angles from accelerometers and leg and bucket position data from potentiometers.

Back End

The back end system includes an XBee module that receives packets from the driver. Serial data received by the XBee module is interpreted to determine which motors to operate and how to operate them. Data is relayed from the XBee to the secondary Propeller and then to the primary Propeller that processes commands for the motor drivers. This Propeller translates the data and updates the robot's state. This state determines the speeds and directions for simpler motor tasks. The more complex motor functions, the arms and digging mechanism, are controlled by PID algorithms. Digging movement and robot velocity updates are translated into simultaneous serial byte commands that coordinate motor driver outputs. The Propellers communicate with each other, receive data from the XBee, and send data to the Sabertooth motor drivers through Spin programs - a language written specifically for the Propeller chips to ensure full compatibility, as well as efficiency.

Front End

The robot is controlled wirelessly from the driver station. A driver operates the robot using dual joystick controllers with the axes and buttons mapped to robot functions, e.g. strafing, turning, and digging. These inputs are read from a Java program, translated into a fourteen byte array representing the state of the joystick, and sent to the robot's XBee receiver over Wi-Fi. Transmission occurs immediately if the state of the joystick is changed; otherwise, the transmission is sent periodically every second. Transmission is done using TCP to minimize errors and so that the driver station is aware when a transmission fails.

The driver station consists of a laptop running a Java program to read two USB controllers and transmit commands over ethernet to a router (Figure 19). The router then relays the data over Wi-Fi to the XBee on the robot.

Figure 19. Operator Interface with Dual Joystick Controllers

In order to send data from the driver station, TCP socket programming is used to serially send data to the XBee. These data packets are then unpackaged and sent directly to the microcontrollers. Although the XBee is able to receive commands via both the User Datagram Protocol (UDP) and TCP protocols, a TCP setup was chosen because it provides a more reliable data transfer. UDP transmits data but does not verify reception of sent packets. TCP requires the receiver to transmit an acknowledgment of data reception to the transmitter. Commands sent through packets by the TCP server contain header information specifying the IP address of the chip and the type of command. Commands can range from setting digital I/O pins, sending serial data, or remotely upgrading the firmware of the XBee, but most commands consist of controller commands sent as serial data that contains instructions for the movement of the robot.

The controller program is currently a half-duplex setup. The driver station sends data to the robot but does not receive anything from it. The Java program supports multithreaded operation to send command data and receive status data. These threads include packet sender/receivers, camera handlers, and keyboard/joystick handlers. A GUI was built on top of these interfaces to provide the controlling user with visual feedback as shown in Figure 20 below.

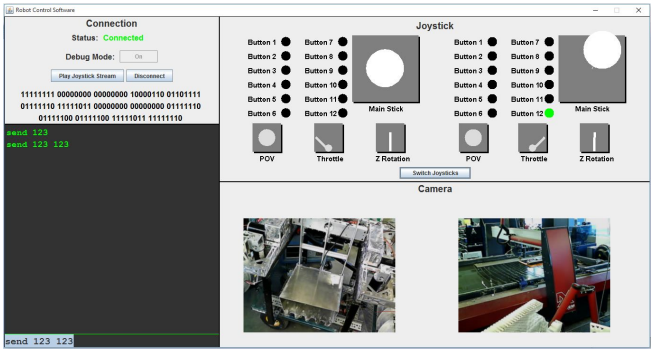

Figure 20. Visualization of Data Flow and Operator Interface

System Integration

Manufacturing

In order to manufacture the components required for mechanical subsystems of the robot, the team took advantage of a number of resources available at Lacy Hall at the University of Virginia, a machine shop free to use for undergraduate students. Available resources include a 3-axis Computer Numerically Controlled (CNC) Vertical Milling Center (VMC), a CNC lathe, a CNC waterjet cutter, and a number of other machining tools. As a result, students are afforded wide flexibility in the design of aluminum and steel robot components. After raw materials are acquired (typically in the form of aluminum sheets/slabs and steel rod), machining of each component or part will take between 30 minutes to two hours, depending on the complexity of the part, and the number of failed attempts.

Mechanical and Electrical Interface

Some of the mechanical changes implemented on the robot rippled through and affected other subsystems. The removal of one of the gearboxes inside the screws changed the way motor drivers were wired to the CCL Industrial Motor (CIM) motors. The dead axle around which each screw rotates has power and ground wires coming out of each side from each CIM motor in order to connect to the motor drivers located on top of the chassis of the robot.

The redesigned power distribution hinges helped make the overall wiring of the robot much more organized and central, as well as safer. Previously, the power and ground buses were separated into two different buses that were each electrically connected to power and ground respectively, coming from the batteries. The new design, combines both the power and ground buses into a single mount separated by a plastic casing in order to isolate both buses from each other, prevent short circuits, and protect them from dust.

Testing

Robot locomotion has undergone minor changes and so is functionally sound as verified in previous years.

As for the excavator system, when tested with a small sample of BP-1 already in possession of the team, the half-inch aluminum mesh installed on the back of the bucket appeared to perform well. Although, due to the ability of BP-1 to pack easily, the mesh alone was not sufficient to completely separate out the subsurface gravel. The team will conduct further testing with the new excavator modifications as mentioned in the Excavator Modifications section.

Integrated automation testing will also be conducted before competition in May, 2018.

Project Management

Budget

The approximate cost breakdown for each major system on the robot is shown in Table 2. The miscellaneous costs refer to the purchase of additional sensors and mechanical components that came about from prototyping and experimenting.

Table 2. Cost Breakdown

Item	*Cost ($)*
Mechanical System	2030
Electronic System	1050
Miscellaneous	1090
Total	4170

Schedule of Work

The tentative schedule of important tasks which guided the design process for the 2017-2018 academic year is outlined in Table 3.

Table 3. Year Round Schedule

Tasks	*Deadlines*
Analysis of bucket vs auger	08/20/17
Screw gearbox redesign	08/20/17
Power distribution redesign	11/01/17
Power distribution manufacture	12/01/17
Circuit board redesign	12/01/17
Leg clamp design	12/01/17
Machine training sessions	01/12/18
Leg clamp manufacture	01/12/18
Machine screw gearbox parts	02/12/18
Electronics box redesign	02/01/18
Automation prototypes	03/01/18
Electronics box manufacture	03/01/18
Mechanical system integration	03/01/18
Circuit board reprint and outfitting	03/01/18
Wiring of entire robot	03/01/18
Excavator prototype design	03/01/18
Excavator prototype	04/01/18
Automation integration	04/01/18
Electrical system integration	04/01/18
Integrated testing	05/01/18

Task Delegation and Management

The team adhered to the task breakdown outlined in Table 4. Additionally, team members reported progress and discussed setbacks during weekly team meetings.

Table 4. Task Breakdown

Member	*Tasks*
Maria	Machine gearbox parts
Henry	Building and testing gearbox, propeller code
Kendall	Machine gearbox parts, bucket
Ian	Machine gearbox parts, electronics box, power distribution system
Samreen	Funding applications, excavator prototype, automation
Cesar	Wiring, automation
Cassie	Circuit Board, automation
Hua	Leg locking signal, wiring
Assad	Java side code- controller
Haley	Excavator bearing block, excavator prototype
Daniel	Visual tracking, java side code
Leslie	Sponsorship, outreach
Robert	Automation
Cristion	Leg clamps, excavator prototype

References

[1] "The Engineering Design Process." 2018. sciencebuddies.org/science-fair-projects/engineering-design-process/engineering-design-process-steps. Accessed: April 10, 2018.

[2] Belleville, Richard et al. 2015. The University of Alabama, Astrobotics, 2015 Systems Engineering Paper.

[3] NASA's Ninth Annual Robotic Mining Competition Rules and Rubrics, Kennedy Space Center. 2018. www.nasa.gov/sites/default/files/atoms/files/2018_rulesrubrics_partiii.pdf. Accessed: April 6, 2018.

[4] Image Gallery: helix angle calculation. 2017. keywordsuggest.org/gallery/87303.html. Accessed: April 10, 2018.

Appendix

Screw Propulsion Efficiency Analysis

The screw propulsion converts the rotational motion of each of the two screws into the linear motion of the robot chassis.

In the case of purely forward motion, the tangential motion of the outer surface of the screw against the sand is converted by the screw threads into axial motion along the length of the screws, with some energy loss due the friction associated with pushing against the regolith.

By "unwrapping" the cylindrical screw face we can simplify the problem of efficiency by modeling as a weighted object being slid up an inclined plane with friction, where the driving force is perpendicular to the upwards motion of the block. It can be shown that the force required to support the downward force on the "block" is equal to Eq. 1, where W is the downward force, θ is the angle of the incline, and ϕ is the friction angle, defined to be

Eq. 1 $$F_{dr} = W * \tan(\theta + \phi)$$

To determine efficiency (Eq.4), the work done by the driving force, work "input", (Eq. 2) and the work done against gravity on the block, work "output",(Eq. 3) where l is distance travelled along the ramp, must be plugged into Eq. 1.

Eq. 2 $$W_{in} = F_{dr} * l * \cos(\theta)$$

Eq. 3 $$W_{out} = W * l * \sin(\theta)$$

Eq. 4 $$\frac{W_{out}}{W_{in}} = \frac{\tan(\theta)}{\tan(\theta + \phi)}$$

This is the equation for the efficiency of our system. Generalizing back to the screw propulsion system, theta is the "lead angle", B of the screw threads, as displayed below [4].

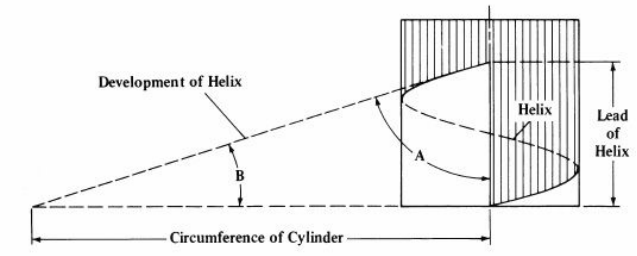

The partial derivative of this function with respect to θ, derives an equation (Eq. 5) for the ideal lead angle for a given friction angle, ϕ.

Eq. 5 $$\theta_{opt} = 45 - \frac{\phi}{2}$$

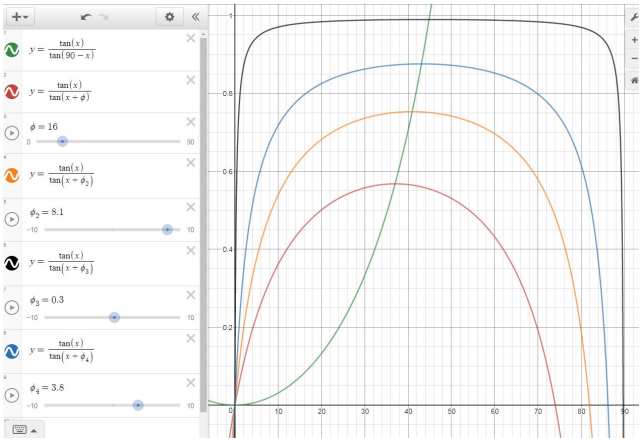

Figure 21. Efficiency curve (green) increases as lead angle increases.

To a reasonable approximation, the coefficient of friction in the context of a screw pushing through sand is the ratio of the drag force to the normal force of a plate pressed down upon and dragged across the surface of packed regolith.

Using simple equipment and a small sample of BP-1 regolith simulant, an experiment to determine the coefficient of friction as previously defined was conducted; thereby solving for an ideal lead angle for our screw-propulsion design.

Three measurements were performed with varying weights of aluminum plate dragged across the surface of a small sample of regolith using an analog force gauge. Measurements for the coefficient of friction and corresponding ideal lead angles are as follows:

Table 5. Ideal Lead Angles for Varying Friction

Coefficient of Friction	*Lead angle with Maximum Efficiency (deg)*
0.43	33
0.48	32
0.52	31

As shown above, all of the measured values place an ideal lead angle somewhere between 30 and 35 degrees.

Due to the way in which the screws are manufactured, the lead angle will actually vary from the innermost point (nearest to the cylinder) to the outer edge. Therefore it was decided to manufacture the screws with an approximately 36 degree "internal" lead angle, which makes the lead angle about 28 degrees at the thread's outermost edge.